

## Chemically-Triggered Synthesis, Remodeling, and Degradation of Soft Materials

Xiaolong Sun, Malgorzata Chwatko, Doo-Hee Lee, James  
Bachman, James F. Reuther, Nathaniel A. Lynd, and Eric V. Anslyn

*J. Am. Chem. Soc.*, **Just Accepted Manuscript** • DOI: 10.1021/jacs.9b12122 • Publication Date (Web): 03 Feb 2020

Downloaded from [pubs.acs.org](https://pubs.acs.org) on February 3, 2020

### Just Accepted

“Just Accepted” manuscripts have been peer-reviewed and accepted for publication. They are posted online prior to technical editing, formatting for publication and author proofing. The American Chemical Society provides “Just Accepted” as a service to the research community to expedite the dissemination of scientific material as soon as possible after acceptance. “Just Accepted” manuscripts appear in full in PDF format accompanied by an HTML abstract. “Just Accepted” manuscripts have been fully peer reviewed, but should not be considered the official version of record. They are citable by the Digital Object Identifier (DOI®). “Just Accepted” is an optional service offered to authors. Therefore, the “Just Accepted” Web site may not include all articles that will be published in the journal. After a manuscript is technically edited and formatted, it will be removed from the “Just Accepted” Web site and published as an ASAP article. Note that technical editing may introduce minor changes to the manuscript text and/or graphics which could affect content, and all legal disclaimers and ethical guidelines that apply to the journal pertain. ACS cannot be held responsible for errors or consequences arising from the use of information contained in these “Just Accepted” manuscripts.

# Chemically-Triggered Synthesis, Remodeling, and Degradation of Soft Materials

Xiaolong Sun,<sup>†</sup> Malgorzata Chwatko,<sup>‡</sup> Doo-Hee Lee,<sup>‡</sup> James L. Bachman,<sup>‡</sup> James F. Reuther,<sup>§</sup> Nathaniel A. Lynd,<sup>\*,‡</sup> and Eric V. Anslyn<sup>\*,‡</sup>

<sup>†</sup>The Key Laboratory of Biomedical Information Engineering of Ministry of Education, School of Life Science and Technology, Xi'an Jiaotong University, Xi'an, 710049, P.R. China.

<sup>‡</sup>Department of Chemistry/McKetta Department of Chemical Engineering, University of Texas at Austin, Austin, Texas, 78712, United States of America.

<sup>§</sup>Department of Chemistry, University of Massachusetts Lowell, Lowell, Massachusetts, 01854, United States of America.

**KEYWORDS:** *Soft materials; click reaction; polymer synthesis; architecture remodeling; chemical degradation;*

**ABSTRACT:** Polymer topology dictates dynamic and mechanical properties of materials. For most polymers, topology is a static characteristic. In this article, we present a strategy to chemically trigger dynamic topology changes in polymers in response to specific chemical stimulus. Starting with a dimerized PEG and hydrophobic linear materials, a lightly cross-linked polymer, and a cross-linked hydrogel, transformations into an amphiphilic linear polymer, lightly cross-linked and linear random copolymers, a cross-linked polymer, and three different hydrogel matrixes, were achieved via two controllable cross-linking reactions: reversible conjugate additions and thiol-disulfide exchange. Significantly, all the polymers, before or after morphological changes, can be triggered to degrade into thiol- or amine-terminated small molecules. The controllable transformations of polymeric morphologies and their degradation heralds a new generation of smart materials.

## INTRODUCTION

Stimuli-responsive polymers that are capable of adapting their structure, constitution, and reactivity on receiving an external stimulus have been emerging in various fields of study, such as biology, medicine, and manufacturing.<sup>1-4</sup> Currently, the control of their properties has been limited to single chemical functional group interchanges, and very limited structural/morphological changes. Similarly, degradable polymers are an important goal within polymer science, and have been used in a wide range of applications spanning medicine and drug delivery, to microelectronics and environmental protection.<sup>5</sup> In 2018, Lamb *et al.* reported that a billion plastic items are entangled on coral reefs across the Asia-Pacific.<sup>6</sup> Thus, it is increasingly critical that plastics and other polymers be triggered to degrade at will.<sup>7</sup>

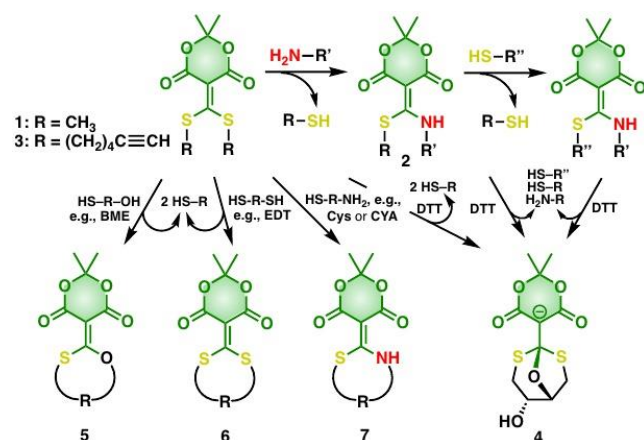
The physical properties of polymers are strongly dependent on several features: their molecular weight distribution, tacticity, topology, chemical functionality, and density of cross-linking.<sup>8</sup> It is rare that these features can be triggered to change by altering the bonding patterns within the backbone structure, as well as changing cross-linking group functionality, and thereby manipulate material properties. To realize transformations of macromolecular topology, exploiting the re-

versibility and orthogonality of dynamic covalent chemistry is useful because these reactions enable independent control over differing functional groups in a single chemical system.<sup>9-12</sup> As alluded to above, if the orthogonal interactions can be manipulated under physiological conditions (*i.e.* in neutral aqueous media), they could lead to new therapeutic materials platforms. Further, if the molecular architecture can be morphed under mild conditions, and with the ability to disassemble the soft materials into small molecules on demand, controllable material properties and triggered biodegradation are within reach. Each of these features is described herein.

In the pursuit of such materials, Sumerlin reported that macromolecular metamorphosis via reversible Diels-Alder transformations of polymer architectures can be achieved in organic media at high temperature over the period of few days.<sup>13-14</sup> This exploration of topological interchange was an important step-forward because a single system could be converted to several macromolecular architectures depending upon reaction conditions. However, the use of elevated temperatures, organic solvents, and the lack of polymer degradation following transformation, limits the applications that can be envisioned.

“Click chemistry” is a term used to describe reactions

that are high yielding, wide in scope, and create byproducts that can be easily removed.<sup>15-17</sup> The Cu(I)-catalyzed Azide/Alkyne Cycloaddition (CuAAC) 'click' reaction has been used extensively in the field of polymer science.<sup>18-20</sup> Recently, our group reported an alternative click strategy, and an associated chemically-triggered "declick", which involves the coupling of amines and thiols via conjugate acceptor **1** that functions in both aqueous and organic media.<sup>21-22</sup> (Scheme 1). The two thioethers in **1** can be released using various reagents,<sup>23</sup> and amine/thiol conjugates such as **2** could be declicked with dithioltreitol (DTT). Noticeably, decoupling of conjugate acceptor **1** releases two equivalents of thiol which can facilitate thiol-disulfide exchange reactions.<sup>23-25</sup> Thus, we envisioned the use of structures such as **1** to couple and decouple amines/thiols in polymers,<sup>26</sup> as well as facilitate disulfide dynamic exchange, as two reversible covalent bonding interactions for independent control of polymer morphology. With these reactions in mind, we pursued linear polymers and cross-linked networks creation, along with chemically-triggered metamorphosis and degradation. The dramatic topological manipulations reported herein, and associated changes in physical properties, induced by chemically-triggered transformations, represent a promising approach to generate tunable 'smart' materials.



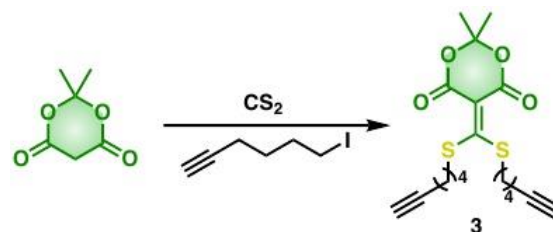
**Scheme 1. A general schematic of the coupling-decoupling reactions exploited herein.** The addition of an amine to **1** or **3** leads to formation of **2** through thiol release. Next, thiols can be scrambled using structures such as **1** or **2** with varying R-groups. The addition of various reagents release thiols and amines in aqueous conditions and can create species **4**, and the generalized structures **5**, **6**, and **7**, each with distinctive UV-Vis  $\lambda_{\max}$  values. (**4**: 250 nm, **5**: 290 nm, **6**: 330 – 350 nm, and **7**: 280 – 300 nm)

## RESULTS AND DISCUSSION

### New conjugate acceptor (CA) and clicking-declicking reactions

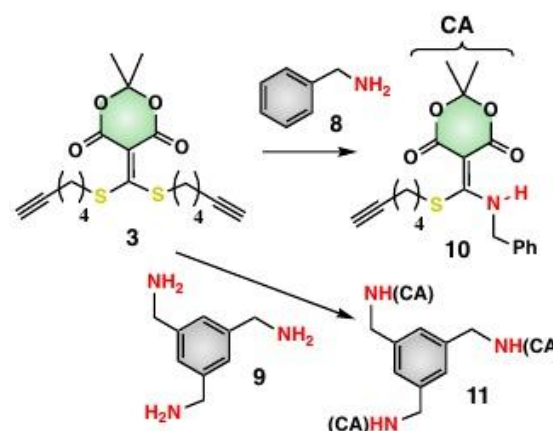
The core unit and basis for topological versatility for the polymers and gels was the conjugate acceptor **3**, which was synthesized from Meldrum's acid, carbon disulfide and 6-iodo-1-hexyne in DMSO at room temperature in

an analogous manner to **1**<sup>21, 27</sup> (Scheme 2, Fig. S1-S3). This subunit was the central, modifiable linker that was used in coupling or cross-linking polymer entities that allows for amine/thiol scrambling or disulfide exchange to chemically trigger morphological changes of the polymer/gel and subsequently "declick" degradation.

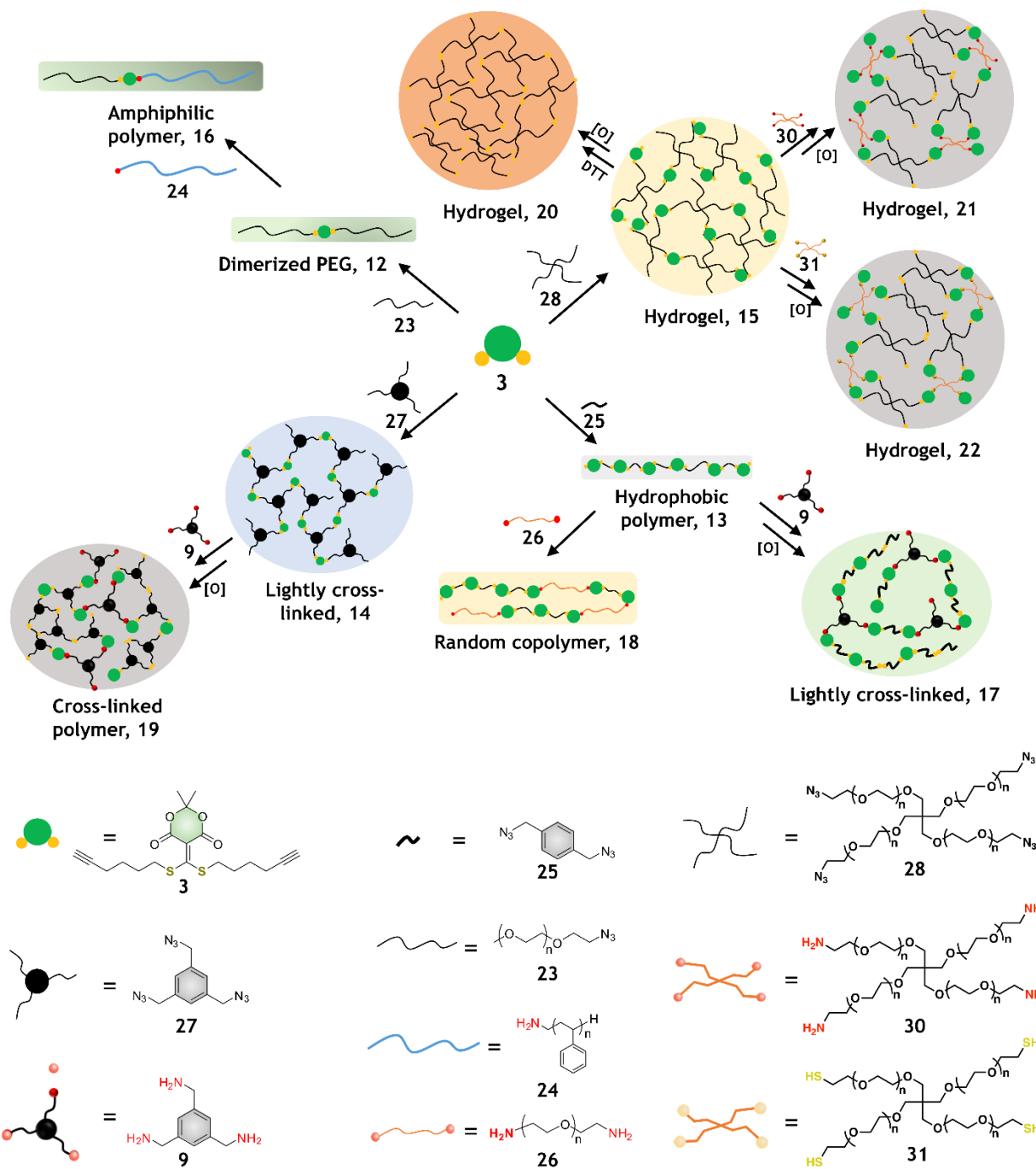


**Scheme 2.** Synthesis of the conjugate acceptor **3**

To generate characteristic spectroscopic signals that would allow us to monitor the transformations of the polymers and gels, we analyzed the spectral differences of the chromophores involved in the clicking and declicking reactions of **1** with small molecules via UV-Vis spectrophotometry. The vinylogous thio-, oxo-, and amino-derivatives shown in Scheme 1 all have distinct absorbance spectra. For example, the reaction of **3** in phosphate-buffered saline (PBS) with DTT,  $\beta$ -mercaptoethanol (BME), ethanedithiol (EDT), cysteine (Cys) and cysteamine (CYA), gave distinguishable UV-Vis absorbance spectra. The  $\lambda_{\max}$  for **3** was at 350 nm, while reagent-induced declicking led to blue-shifted spectra and different  $\lambda_{\max}$  values depending on the structure of the cyclized products: DTT (250 nm, a tricyclic product, **4**),<sup>28</sup> BME (290 nm, **5**), EDT (330 nm, **6**), Cys or CYA (280 nm, **7**) (Fig. S4). The relative speed of decoupling was DTT > BME > EDT ~ CYA > Cys. Thus, the chemical group interchanges involved in the polymer/network topological changes could be monitored by simple UV-Vis absorbance spectroscopy, and the rate of decoupling could be controlled, if desired. As described below, the  $\lambda_{\max}$  values allowed us to follow the extent of chemical functional group interchange.



**Scheme 3.** The reactions between **3** and amine derivatives



**Scheme 4. Schematic representation of the polymer synthesis and topological changes achieved via click-declick chemistry and disulfide-thiol scrambling.** Dimerized PEG (12) and hydrophobic linear polymer (13), lightly cross-linked polymer (14), and hydrogel (15) were synthesized via CuAAC. New amphiphilic linear polymer (16), lightly cross-linked (17), random copolymer (18), cross-linked polymer (19) and hydrogels (20, 21, 22) were created via amine scrambling using the conjugate acceptor core of 3, and/or thiol-disulfide reactions. Note: Given the potential hazards of poly(azide) compounds, the reactions were carried out in the fume hood, treated carefully, stored and used in safe places.<sup>29</sup>

Next, LC-MS was employed to monitor the reactions between 3 and small molecular amines, such as benzyl amine (8) and 1,3,5-triaminomethylbenzene (9), to confirm the expected mono-thiol displacements. After five minutes, LC-MS peaks corresponding to complete product formation (10 and 11, CA = conjugate acceptor derived from 3) were identified for both amines (Scheme

3, Fig. S5). Further, upon addition of a declicking trigger (DTT), the LC-MS peak corresponding to 10 and 11 vanished and a peak indicative of the tricyclic product 4 was observed (Fig. S6), confirming that 3 retained similar chemical properties to 1 in the context of click and declick reactions.

## Polymer design, analysis and transformation. An overview

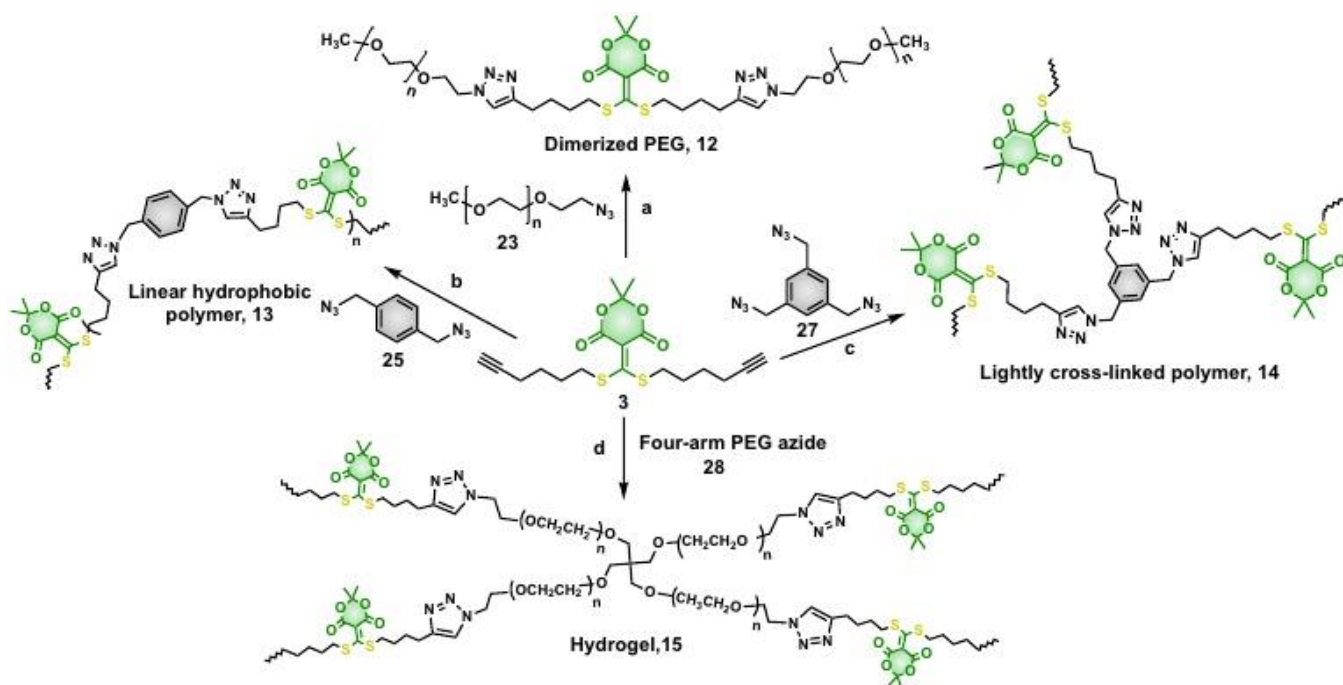
To start, we created four polymer types by using standard CuAAC reactions: dimerized PEG **12**, linear hydrophobic **13**, hyper-branched **14**, and a cross-linked hydrogel **15** (Schemes 4 and 5). There were several reasons to choose these four architectures as our starting point. Linear polymers such as polyethylene, nylons, and polyesters possess high densities, high tensile strengths, and high melting points.<sup>30</sup> Lightly cross-linked polymers have been widely applied in many applications, such as light emitting materials, biomaterials, and composites.<sup>31</sup> Hydrogels are commonly used scaffolds in tissue engineering, drug delivery, as well as sensing.<sup>32-33</sup> Important for our triggered morphology changes, these four starting polymeric architectures contain repeating core conjugate-acceptors analogous to **1** and **3**. These acceptors could undergo reactions with amine-terminated polymers or branched monomers via the click reaction that releases a thiol. In turn, the released thiols can be used in oxidation/reduction reactions through disulfide exchange. Thus, starting with structures **12-15**, an amphiphilic linear **16**, a lightly cross-linked homopolymer **17**, a random copolymer **18**, a cross-linked polymer **19**, and hydrogels **20**, **21**, **22** were generated by amine scrambling and thiol disulfide formation (Scheme 4, and Table S1). Furthermore, all the polymeric architectures — before or after morphological changes — were degraded into small molecules or homopolymers induced by declick triggers, hence presaging potential ap-

plications such as plastic remediation, drug delivery, tissue engineering, or microelectronics.<sup>2, 5</sup>

## Dimerized PEG transformation to aggregated structures

The dimerized PEG **12** was formed by CuAAC of poly(ethylene glycol) methyl ether azide (**23**,  $M_n$  ca. 1,000 g mol<sup>-1</sup>) and **3** in a *tert*-butanol/water mixture (Scheme 5). Proton NMR spectroscopy (Fig. S7) displayed the formation of triazole moieties and LC-MS spectrum (Fig. S8, S9) showed the product with mass/charge ratio ( $m/z$ ) = 2565.40 for [**12**+H]<sup>+</sup>, and 1327.24 for [**12**+2H]<sup>2+</sup>. Next, gel permeation chromatography (GPC) displayed a shift to a lower elution time for **12** compared to **23** (Fig. 1E), indicating the successful click of **23** with **3**.

To transform **12** to an amphiphilic polymer, amine-terminated polystyrene **24** ( $M_n$  ca. 5,000 g mol<sup>-1</sup>) was utilized to scramble one thiol of **12** to generate **16** (Scheme 4, and Fig. S10). To monitor the transformation, UV-Vis absorbance was used, which revealed a blue-shifted ratiometric signal corresponding to product formation. Specifically, the shift in absorbance of the bis-vinylous thiol ester, as found in structure **1** (as in **6**) ( $\lambda_{max}$  = 330 - 350 nm), relative to an amine/thiol version of the conjugate acceptor, as found in structure **2** (as in **7**) ( $\lambda_{max}$  = 310 nm), indicated the formation of polymeric product **16** (Fig. 1A and S11). In GPC analysis, **16** displayed a lower retention time and higher molecular weight ( $M_n$  = 5,800 g mol<sup>-1</sup>) with  $D$  = 1.3 (Fig. 1E). Subsequently, **16** was in-



**Scheme 5. Synthesis of the initial set of subunits.** Reagents and conditions: a. CuSO<sub>4</sub>·5H<sub>2</sub>O, sodium ascorbate, *tert*-butanol:H<sub>2</sub>O = 1:1 (vol), 20 °C; b. CuI, tris(benzyltriazolylmethyl)-amine (TBTA), sodium ascorbate, THF:DMF:H<sub>2</sub>O = 2:2:1 (vol), 20 °C; c. CuI, TBTA, sodium ascorbate, THF:DMF:H<sub>2</sub>O = 1:1:1 (vol), 20 °C; d. CuSO<sub>4</sub>·5H<sub>2</sub>O, sodium ascorbate, *tert*-butanol:H<sub>2</sub>O = 1:1 (vol), 20 °C.

investigated using DLS to evaluate the size and amphiphilic properties (Fig. 1F, S12 and S13). The correlation in size determined by DLS in aqueous solution (ca. 90 nm) suggests that **16** existed in assemblies.<sup>34-36</sup> Thus, a hydrophilic freely aqueous soluble compound was triggered to generate aggregation in-situ by an exchange of a single block unit.

### Hydrophobic polymer transformations to lightly cross-linked and amphiphilic co-polymers

The linear hydrophobic polymer **13** was obtained through step-growth CuAAC polymerization between **3** and 1,4-di(azidomethyl)benzene **25**, which afforded a yellow solid ( $M_n = 5,300 \text{ g mol}^{-1}$ ,  $D = 1.35$ ) after precipitation and purification. (Scheme 5, Fig. S14). Simple addition of 1,3,5-triaminomethylbenzene **9** to **13** resulted in a distinctive change in the polymer backbone as well as cross-linking. UV-Vis time-kinetics displayed a blue-shift due to amine scrambling (*i.e.* analogous of **1** to **2**), giving a clean isosbestic point at  $\lambda = 325 \text{ nm}$  (Fig. 1B). <sup>1</sup>H NMR spectroscopy titrations of **13** with **9** demonstrated

amine-induced scrambling and complete thiol release (Fig. S15). This topological change releases dangling thiols in the polymer, and we took advantage of this to further cross-link the material. Thus, oxidation of the dangling thiols to disulfides was performed by addition of  $\text{H}_2\text{O}_2$ , generating lightly cross-linked polymer **17** ( $M_n = 21.0 \text{ kg mol}^{-1}$ ,  $D = 1.18$ , Fig. 1H, Table S2 and Fig. S16). In Figure 1H, the prominent shoulders are likely due to smaller molecular weight polymers/oligomers with different extents of cross-linking. The approximate molecular weight of these shoulders is 200 g/mol and below. To further determine the role of  $\text{H}_2\text{O}_2$ , we checked if sulfoxides were formed by oxidation of the thioethers of the Meldrum's acid derivatives. LC-MS was used to monitor the reaction between **1** and  $\text{H}_2\text{O}_2$ . This was conducted using the same conditions used in creating polymer **17**, and there was no chemical reaction (Fig. S17). Also, an additional experiment was carried out with an excess of  $\text{H}_2\text{O}_2$ , and again no reaction was found. All the above data shows that polymer **17** was constructed by two covalent attachments, one through

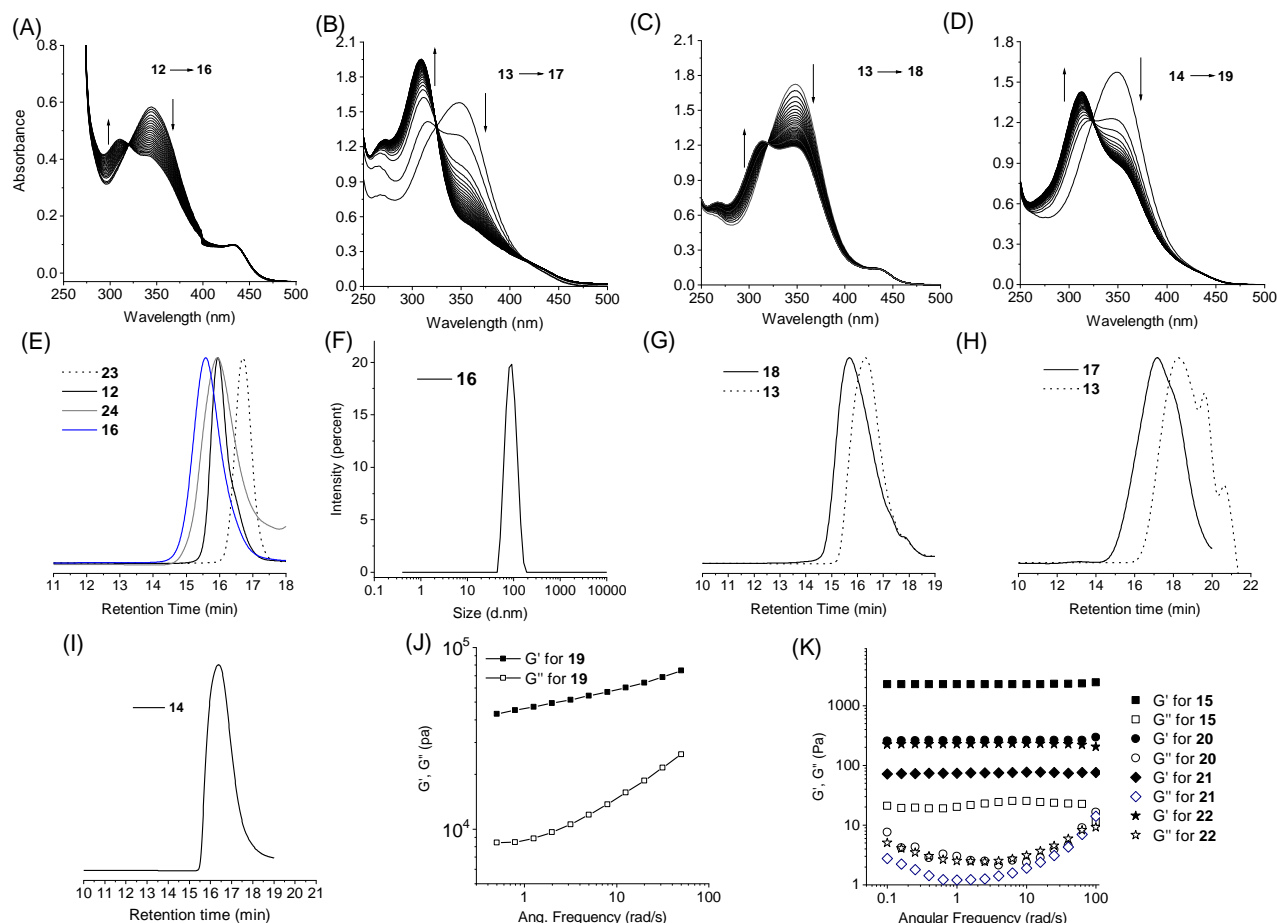
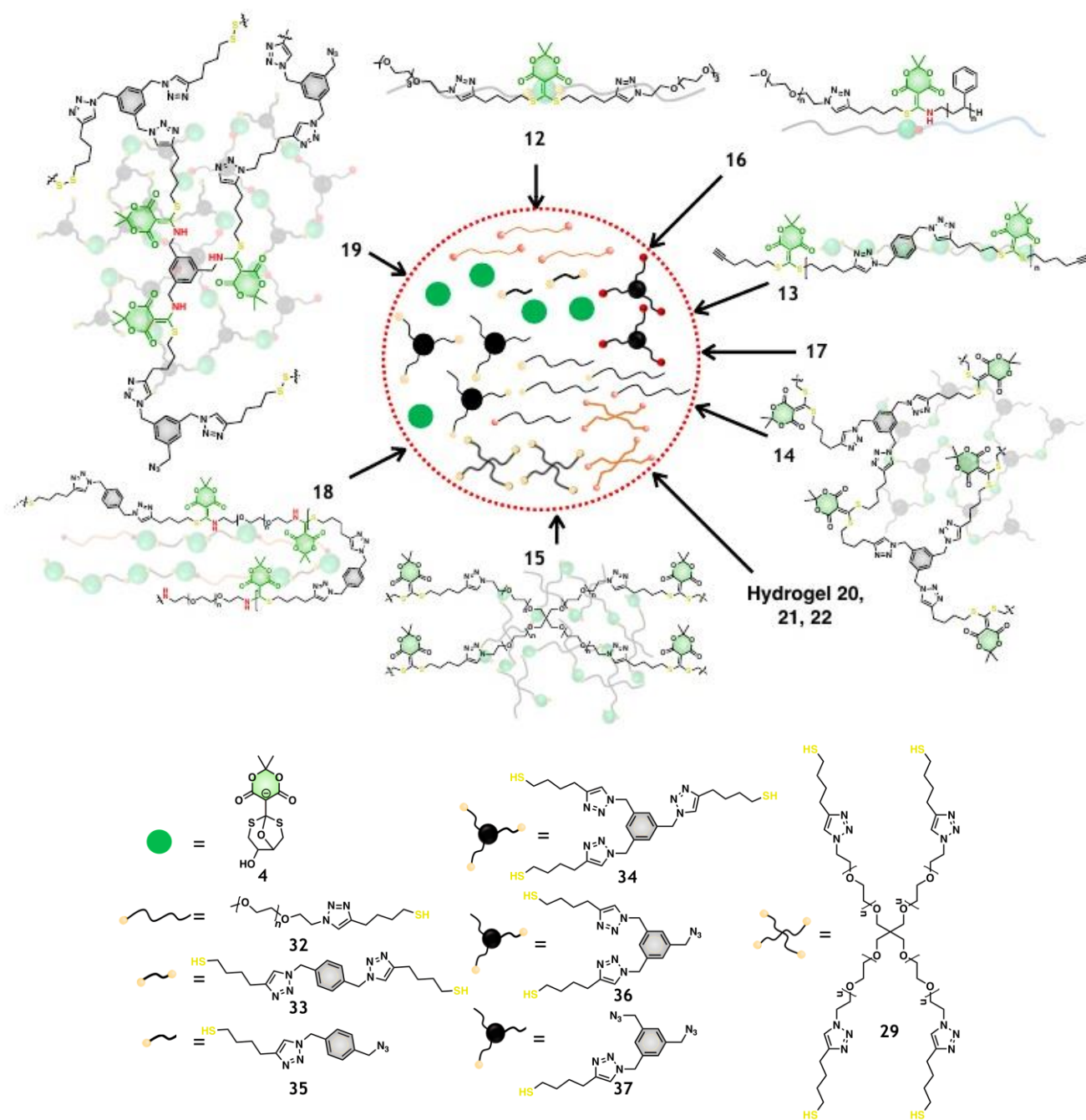


**Figure 1.** UV-Vis absorbance time kinetics, GPC, and rheometry for the polymer remodeling. (A) **12** (0.25 mg/mL) to **16** using amine terminated polystyrene **24** (1.0 mg/mL); (B) **13** (0.4 mg/mL) to **17** using 1,3,5-triaminomethylbenzene **9** (20  $\mu\text{M}$ ); (C) **13** (0.2 mg/mL) to **18** using PEG diamine **26** (0.2 mg/mL); (D) **14** (0.14 mg/mL) to **19** using **9** (41  $\mu\text{M}$ ) before adding hydrogen peroxide. The time kinetics were run in chloroform every 20 mins for (A); every 10 mins for (B) and (D); every 30 mins for (C); (E) GPC for **12**, **16**, **23** and **24** in chloroform; (F) DLS for **16** in water; (G) GPC for **13** and **18** in chloroform; (H) GPC for **13** and **17** in DMF (containing 0.01 M LiBr); (I) GPC for lightly cross-linked polymer **14** in chloroform; (J) Storage modulus  $G'$  and loss modulus  $G''$  for cross-linked polymer **19**; (K) Storage modulus  $G'$  and loss modulus  $G''$  for swelled hydrogel **15**, **20**, **21** and **22** in HEPES buffer.



**Scheme 6. Schematic depiction of polymer degradation induced in the presence of DTT or tris(2-carboxyethyl)phosphine (TCEP)/ethanolamine in neutral HEPES buffer.** The degradation process was triggered either by the cyclization between a bis-vinyllogous derivatives of **3** with DTT, or disulfide cleavage by reduction with TCEP, or ethanolamine-induced decoupling of structures such as **1**, respectively.

the thiol/amine conjugate such as **2**, and the other through disulfide bonds. Thus, we triggered both backbone and cross-linking interchanges from a hydrophobic polymer to a lightly cross-linked network.

In the next transformation, poly(ethylene glycol) diamine **26** ( $M_n = 6,000 \text{ g mol}^{-1}$ ) was used to functionalize **13**, again via thiol displacement. Following the reaction between **13** and **26** in 1:1 ratio, product **18** was precipitated from cold methanol. UV-Vis spectroscopy again demonstrated a decrease in the absorbance of 350 nm

and increase at 310 nm (Fig. 1C) while GPC displayed a lower retention time and higher molecular weight ( $M_n = 38.9 \text{ kg mol}^{-1}$ ,  $D = 1.39$ , Table S2) for **18**, indicating the formation of longer random copolymers (Fig. 1G). Additionally, analysis of the  $^1\text{H}$  NMR spectrum (Fig. S18) revealed the presence of peaks corresponding to PEG backbone protons. These data demonstrate successful chemically-triggered remodeling of the linear polymers through amine/thiol scrambling.

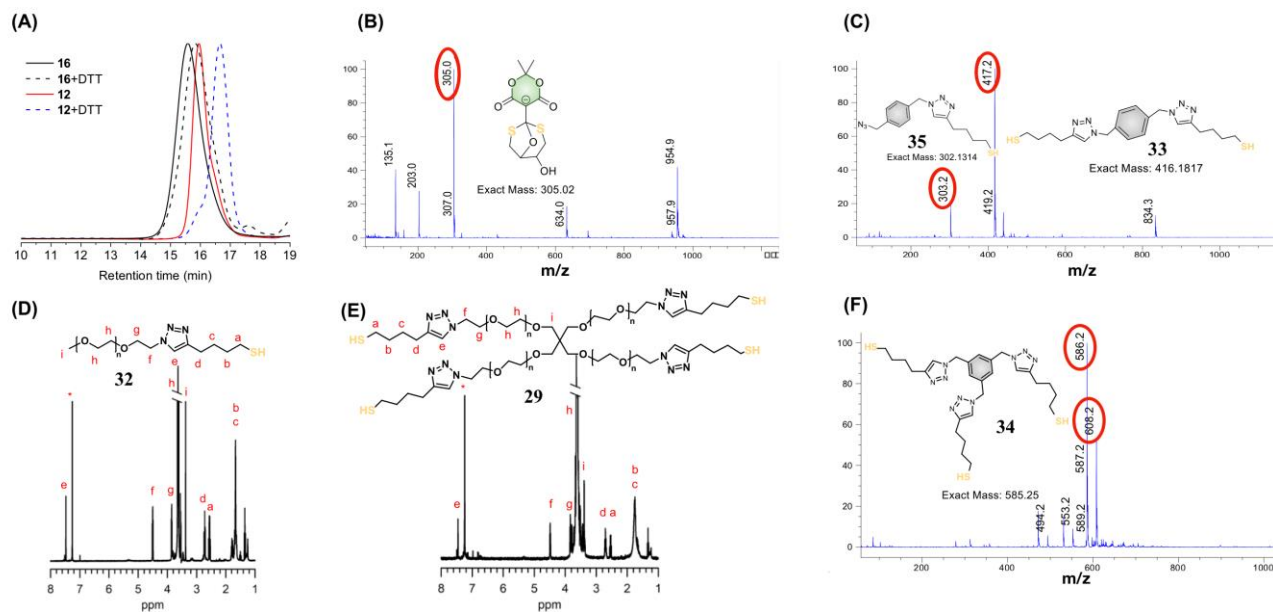


**Figure 2.** GPC, <sup>1</sup>H NMR spectroscopy, and LC-MS for the polymer degradation. (A) GPC of **12** and **16** before and after degradation; (B) Mass spectra for tricyclic product **4** observed in LC-MS; (C) Masses for **33** and **35** observed in LC-MS, resulted from decomposition of **13**, **17** and **18**; (D) <sup>1</sup>H NMR for the thiol-terminated PEG product **32** released from **12**; (E) <sup>1</sup>H NMR for the four-arm PEG thiol **29** degraded from hydrogel **15**; (F) Mass spectra for **34** released from **14** and **19** in LC-MS.

### Lightly cross-linked polymer transformations to cross-linked polymer

Lightly cross-linked polymer **14** was synthesized through the copper-catalyzed click reaction between **3** and 1,3,5-tris(azidomethyl)benzene **27** (Scheme 5, Fig. S19). GPC with multiangle light scattering detection gave the molecular weight for **14** ( $M_n = 14.9 \text{ kg mol}^{-1}$ ,  $\mathcal{D} = 1.16$ , Fig. 1I, Table S2). Using <sup>1</sup>H NMR analysis ala the method of Moore,<sup>37</sup> an approximate degree of branching of 65% was obtained. Similar to the reaction of **12** or **13**, UV-Vis kinetics of the reaction of **14** with the triamine **9** demonstrated a blue shift, and new <sup>1</sup>H NMR spectroscopy resonances appeared in a time-dependent manner (Fig. 1D and S20). The analyses confirmed the remodeling of the architecture and the release of thiol moieties.<sup>38</sup> The product was directly oxidized with H<sub>2</sub>O<sub>2</sub> resulting in a highly cross-linked polymer **19** in a DMF/THF mixture which exists as a gel (Fig. S21). Rheometric tests found the storage modulus ( $G'$ ) to be an average of 5.5 kPa and the loss modulus ( $G''$ ) to be 1.5 kPa on average, slightly increasing with the change of angular frequency in the range of 0.1 – 100 rad/s (Fig. 1J). In summary, lightly cross-linked polymeric backbones were morphed, resulting in gels in situ by simple addition of a cross-linking unit.

### Hydrogel transformations to mono- and double networking hydrogels

In addition to polymers, the strategies discussed here were applied to matrix hydrogels. Initially, hydrogel **15** was synthesized via click reaction between **3** and four-arm poly(ethylene glycol) azide **28** ( $M_n \sim 10.0 \text{ kg mol}^{-1}$ )

in a water/*tert*-butanol mixture (Scheme 5). The volume of the hydrogel was expanded after swelling in water due to the hydrophilic network, (see supplementary material) resulting in a frequency-independent storage modulus of 2.2 kPa (Fig. 1K).

Next, DTT was used to degrade the hydrogel by cleaving the linkage at conjugate acceptor core **3**, leading to the quantitative generation of four-arm PEG thiol **29** (Fig. 2E) in pH 7.3 HEPES (4-(2-hydroxyethyl)-1-piperazine-ethanesulfonic acid) buffer. After removal of **4** and residual DTT by dialysis, the resulting system containing numerous free thiols was cross-linked through disulfide bonds by addition of H<sub>2</sub>O<sub>2</sub>, generating a new networking matrix: hydrogel **20** (Table S1, Fig. S22). Gel **20** demonstrated a softened elastic modulus of only 260 Pa corresponding to lower overall cross-link density (Fig. 1K). Continuing with the theme, we employed four-arm poly(ethylene glycol) amine **30** ( $M_n$  ca. 2.0 kg mol<sup>-1</sup>) to construct hydrogel **21**, using multiple amines separated by long PEG chains that expanded the matrix of the hydrogel through scrambling thiols on the conjugate acceptor. Visibly, hydrogel **15** became a viscous liquid after mixing with **30** for six hours (1:1 ratio to the conjugate acceptor), liberating the thiols along with a noticeable odor. Subsequent addition of H<sub>2</sub>O<sub>2</sub> linked the free thiols as disulfides in a second crosslinking, leading to hydrogel **21** (Fig. S23). Rheometric testing gave an even softer storage modulus (75 Pa) for the swelled hydrogel, which supported our proposed role of **30** to expand the hydrogel matrix. Next, four-arm PEG thiol **31** ( $M_n$  ca. 5.0 kg mol<sup>-1</sup>, 1:1 ratio to the conjugate acceptor) was utilized to morph the matrix of hydrogel **15**, of which the thiols

would exchange between a bis-vinylous thiol esters in **15** and thiol-terminated derivative **31**. Subsequently, released free thiols enabled the second cross-linking through formation of disulfides, generating hydrogel **22** (Fig. S24). With this different cross-linking, the storage modulus became to 230 Pa. Thus, numerous hydrogels of differing physical properties resulting from backbone alternations were readily created via simple mixing of reagents.

Significantly, all of the topological remodeling of the polymer and hydrogel backbones and cross-linkers were performed in neutral aqueous condition at ambient temperature by simply adding new monomers, cross-linkers, polymers or an oxidant. The resulting spatio-temporal regulation of material properties is promising in the applications of drug delivery system, cells encapsulation, and cell migration.

### Macromolecular degradation into small molecules

Remodeling and transforming polymeric architectures via chemically-triggered synthesis has been described above. Another critical property of a polymer is its ability to degrade, which facilitates controlled removal of plastic pollutants once the material has served its purpose. Further, such triggerable material degradation should hold wide applicability in biomedicine and drug-delivery. As we have stressed throughout, all of the bis-vinylous thiol esters analogous to **1**, bis-vinylous thiol amine structures containing linkages as in **2**, and disulfide bonds, could be decoupled by various chemical reagents. Further, with the co-existence of two or

more crosslinking chemical bonds, we could control and tune the degradation through different declipping reactions.

First, **12** was treated with DTT in HEPES buffer (pH 7.3) for three hours and the solution was then placed in dialysis tubing (1.0 kDa molecular weight cut-off) and suspended in deionized water for 40 hours (changing the solvent every ten hours) to remove small molecules (Fig. S25). The thiol-terminated product **32** was confirmed by <sup>1</sup>H NMR spectroscopy (Fig. 2D) and GPC, where a longer retention time (Fig. 2A) indicated success of the decoupling reactions. Next, **16** was declipped using DTT for 36 hours in HEPES buffer (50% acetonitrile as co-solvent, Fig. S26). After dialysis, GPC data showed that the result had a lower molecular weight (Fig. 2A). Next, polymers **13**, **14**, **17**, **18** and **19** were all processed in HEPES buffer in the presence of DTT (overnight for **13** and **14**; two days for **17** and **18**; five days for **19**). As expected, the polymers containing amine/thiol conjugate acceptors such as structure **2**, were more difficult to decompose than the polymers containing thiol ester conjugate acceptors such as with **1**, due to the amine being less labile as a leaving group. Yet, all species did entirely degrade with DTT. A macroscopic surface-accessible degradation occurred, which can be seen by the naked-eye and analyzed by LC-MS. LC-MS data showed the tricyclic product **4** (Fig. 2B) with a mass/charge ratio ( $m/z$ ) = 305.0 for all polymers declipped by DTT, and bis-thiol terminated derivative **33** released from **13**, **17** and **18** ( $m/z$  = 417.2, Fig. 2C, Fig. S27–S29); three-arm thiol derivative **34** released from **14** and **19** ( $m/z$  = 586.2, 608.2 Fig. 2F,

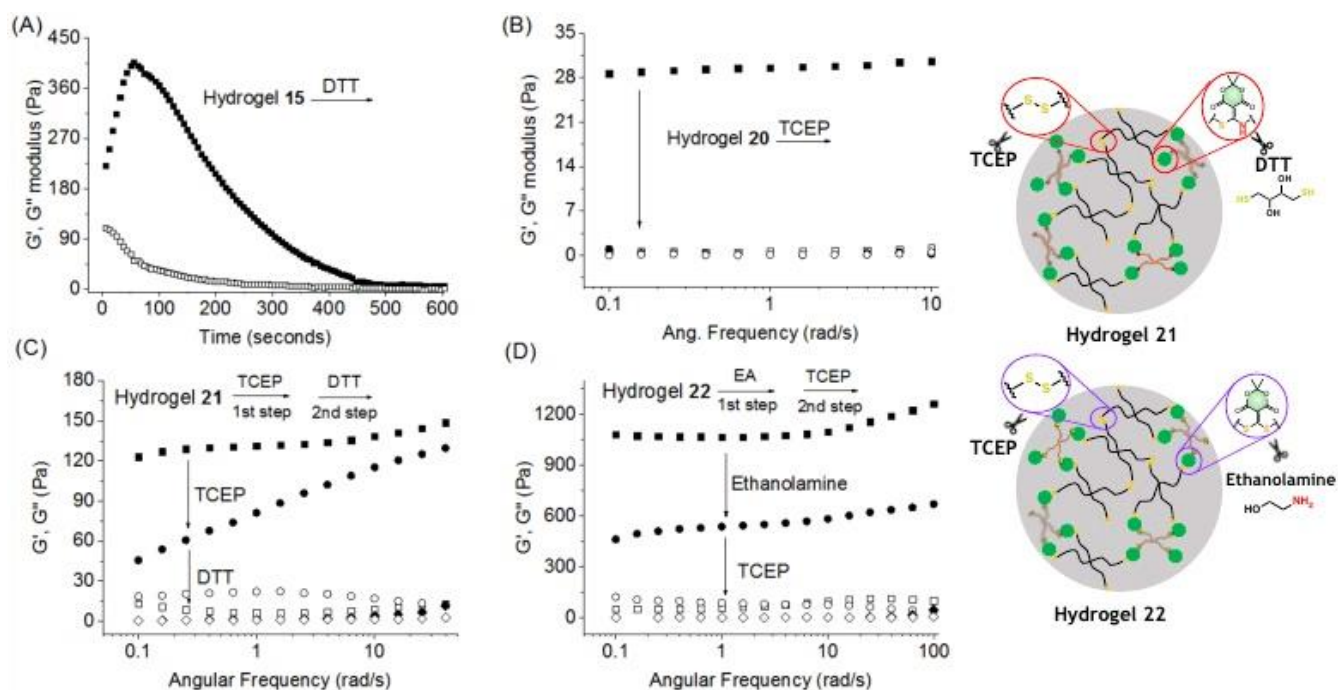


**Figure 3. Monitoring hydrogel degradation by rheometer.** (A) Time-based kinetics for degradation of hydrogel **15** in the presence of DTT; (B) TCEP-induced disulfide reduction for hydrogel **20** degradation; (C) Two cross-linked networks: disulfide bond and amine/thiol conjugate acceptor linked in hydrogel **21** were degraded by TCEP and DTT, respectively; (D) Two cross-linked networks: a bis-vinylous thiol-ester such as **1** and disulfide bond linking hydrogel **22** were degraded by ethanolamine and TCEP, respectively. Storage modulus and loss modulus for hydrogels **20**, **21** and **22** were scanned before and after degradation.

Fig. S30–S31), respectively. We also observed the azide-containing side products **35** and **36**, **37** (Fig. 2C, Fig. S27–S31) from declick reaction mentioned above, due to incomplete CuAAC click reaction.

DTT was also successfully used to declick the hydrogels into small molecules. The 3D network **15** was processed in HEPES buffer in the presence of DTT, and after 20 minutes the yellow gel disassembled, with no disassembly of the control sample without DTT (inset picture in Fig. S32). LC-MS verified the generation of **4** (Fig. S32), and following dialysis, <sup>1</sup>H NMR spectroscopy confirmed formation of **29** (Fig. 2E). Furthermore, kinetic studies from the rheometer displayed a decreasing of the storage modulus ( $G'$ ) due to degradation of hydrogel **15** following addition of DTT, indicating gradual breakage of the matrix (Fig. 3A, Fig. S33). Next, the viscoelasticity of a soft hydrogel **20** (storage modulus  $G' = 28$  Pa) was transformed rapidly into a solution state ( $G' < G''$ ) due to the cleavage of disulfide bonds by tris(2-carboxyethyl)phosphine (TCEP) (Fig. 3B). Following dialysis, the solution state was reversed into a gel under hydrogen peroxide due to the reformation of disulfide bonds (Fig. S34).

The crosslinked matrixes **21** and **22** could also be tuned and controlled by different decoupling reagents. The matrix of hydrogel **21** ( $G' \sim 130$  Pa), containing both the amine/thiol conjugate and disulfide bonds, were tuned separately by TCEP for the reduction of disulfides ( $G' \sim 70$  Pa), and subsequently by DTT for the cleavage of the thiol-amine conjugate analogous to **2** ( $G' \sim 5$  Pa, Fig. 3C and S35). While for hydrogel **22** ( $G' \sim 1000$  Pa), ethanolamine was employed to cut off the bis-vinylous thiol ester core analogous to **1** ( $G' \sim 500$  Pa), and then TCEP was used to reduce the disulfide bonds ( $G' \sim 5$  Pa), decomposing the cross-linked hydrogel entirely into small molecules (Fig. 3D and S36). The tunable and degradable properties of the hydrogels, particularly the ability to tune the two dynamically cross-linked samples under physiological conditions, are potentially applicable in drug delivery systems and tissue bioengineering.

## CONCLUSION

We have demonstrated in macromolecular constructs the versatility of being able to click thiols, and amines and thiols, via structures analogous to **1** to make morphable soft materials. By simply controlling the sequence of addition of monomers, cross-linkers or polymers, we could chemically trigger interconversion of backbone architectures and crosslinks, control polymer morphologies, and alter macroscopic properties, all at ambient temperature in aqueous media. In specific, the reversible conjugate additions inherent in the organic chemistry of **1** and its analogs introduced herein, coupled with thiol-disulfide scrambling, led to very simple approaches that interconvert linear hydrophobic, hydrophilic, and amphiphilic polymers, as well as lightly

cross-linked polymers and hydrogels; further even allowing interconversion of random co-polymers with other lightly cross-linked polymers. In addition, in a facile fashion 4 different hydrogels could be created via manipulating the components allowed to react with structures containing the reactivity of **1**. The choice of amines and thiols used herein are specific to this study, but clearly the possibilities are vast given the numbers of amine and thiol units that can be imagined. Lastly, and potentially just as important, all the soft materials are degradable with various chemical triggers, albeit specifically DTT was used in this study. Owing to the mild reaction conditions and ease of use in a wide variety of applications, this method is expected to have numerous material applications.

## ASSOCIATED CONTENT

This Supporting Information is available free of charge via the Internet at <http://pubs.acs.org>.

Additional experimental procedures and characterization data are provided in the supplementary materials. Materials and Methods, Supplementary Text, Figs. S1 to S35, Tables S1 to S2, Captions for Data S1 to S35, Synthetic preparations.

## AUTHOR INFORMATION

### Corresponding Author

\*anslyn@austin.utexas.edu (E.V.A.);

\*lynd@che.utexas.edu (N.A.L)

### ORCID

Xiaolong Sun: 0000-0003-4003-6924

Doo-Hee Lee: 0000-0002-5116-2064

James F. Reuther: 0000-0001-5611-0290

Nathaniel A. Lynd: 0000-0003-3010-5068

Eric V. Anslyn: 0000-0002-5137-8797

### Notes

The authors declare no competing financial interest.

## ACKNOWLEDGMENT

The authors acknowledge the use of facilities and instrumentation supported by the National Science Foundation through the Center for Dynamics and Control of Materials: an NSF MRSEC under Cooperative Agreement No. DMR-1720595, and NIH grant number 1 S10 OD021508-01. We gratefully acknowledge the support of the Welch Regents Chair (F-0046) to EVA and the Welch Foundation (F-1904) to NAL. XLS thanks the National Natural Science Foundation of China No. 21907080.

## REFERENCES

1. Stuart, M. A. C.; Huck, W. T.; Genzer, J.; Müller, M.; Ober, C.; Stamm, M.; Sukhorukov, G. B.; Szleifer, I.; Tsukruk, V. V.; Urban, M., Emerging applications of stimuli-responsive polymer materials. *Nat. Mater.* **2010**, *9* (2), 101-113.
2. Blum, A. P.; Kammeyer, J. K.; Rush, A. M.; Callmann, C. E.; Hahn, M. E.; Gianneschi, N. C., Stimuli-responsive nanomaterials for biomedical applications. *J. Am. Chem. Soc.* **2015**, *137* (6), 2140-2154.

3. Montero de Espinosa, L.; Meesorn, W.; Moatsou, D.; Weder, C., Bioinspired Polymer Systems with Stimuli-Responsive Mechanical Properties. *Chem. Rev.* **2017**, *117* (20), 12851-12892.
4. Shafranek, R. T.; Millik, S. C.; Smith, P. T.; Lee, C.-U.; Boydston, A. J.; Nelson, A., Stimuli-responsive materials in additive manufacturing. *Prog. Polym. Sci.* **2019**, *93*, 36-67.
5. Delplace, V.; Nicolas, J., Degradable vinyl polymers for biomedical applications. *Nat. Chem.* **2015**, *7* (10), 771-784.
6. Lamb, J. B.; Willis, B. L.; Fiorenza, E. A.; Couch, C. S.; Howard, R.; Rader, D. N.; True, J. D.; Kelly, L. A.; Ahmad, A.; Jompa, J., Plastic waste associated with disease on coral reefs. *Science* **2018**, *359* (6374), 460-462.
7. Christensen, P. R.; Scheuermann, A. M.; Loeffler, K. E.; Helms, B. A., Closed-loop recycling of plastics enabled by dynamic covalent diketoenamine bonds. *Nat. Chem.* **2019**, *11* (5), 442-448.
8. Su, W.-F., Chemical and Physical Properties of Polymers. In *Principles of Polymer Design and Synthesis*, Springer Berlin Heidelberg: Berlin, Heidelberg, 2013; pp 61-88.
9. Scheutz, G. M.; Lessard, J. J.; Sims, M. B.; Sumerlin, B. S., Adaptable Crosslinks in Polymeric Materials: Resolving the Intersection of Thermoplastics and Thermosets. *J. Am. Chem. Soc.* **2019**, *141* (41), 16181-16196.
10. Reuther, J. F.; Dahlhauser, S. D.; Anslyn, E. V., Tunable Orthogonal Reversible Covalent (TORC) Bonds: Dynamic Chemical Control over Molecular Assembly. *Angew. Chem. Int. Ed.* **2019**, *58* (1), 74-85.
11. Cudjoe, E.; Herbert, K. M.; Rowan, S. J., Strong, Rebondable, Dynamic Cross-Linked Cellulose Nanocrystal Polymer Nanocomposite Adhesives. *ACS Appl. Mater. Interfaces* **2018**, *10* (36), 30723-30731.
12. Rowan, S. J.; Cantrill, S. J.; Cousins, G. R.; Sanders, J. K.; Stoddart, J. F., Dynamic covalent chemistry. *Angew. Chem. Int. Ed.* **2002**, *41* (6), 898-952.
13. Sun, H.; Kabb, C. P.; Sims, M. B.; Sumerlin, B. S., Architecture-transformable polymers: Reshaping the future of stimuli-responsive polymers. *Prog. Polym. Sci.* **2019**, *89*, 61-75.
14. Sun, H.; Kabb, C. P.; Dai, Y.; Hill, M. R.; Ghiviriga, I.; Bapat, A. P.; Sumerlin, B. S., Macromolecular metamorphosis via stimulus-induced transformations of polymer architecture. *Nat. Chem.* **2017**, *9*, 817-823.
15. Kolb, H. C.; Finn, M.; Sharpless, K. B., Click chemistry: diverse chemical function from a few good reactions. *Angew. Chem. Int. Ed.* **2001**, *40* (11), 2004-2021.
16. Kolb, H. C.; Sharpless, K. B., The growing impact of click chemistry on drug discovery. *Drug. Discov. Today* **2003**, *8* (24), 1128-1137.
17. Qin, A.; Lam, J. W. Y.; Tang, B. Z., Click polymerization. *Chem. Soc. Rev.* **2010**, *39* (7), 2522-2544.
18. Arslan, M.; Tasdelen, M. A., Click Chemistry in Macromolecular Design: Complex Architectures from Functional Polymers. *Chemistry Africa* **2018**, *2* (2), 195-214.
19. Binder, W. H.; Sachsenhofer, R., 'Click' chemistry in polymer and materials science. *Macromol. Rapid Commun.* **2007**, *28* (1), 15-54.
20. Binder, W. H.; Sachsenhofer, R., 'Click' chemistry in polymer and material science: an update. *Macromol. Rapid Commun.* **2008**, *29* (12 - 13), 952-981.
21. Diehl, K. L.; Kolesnichenko, I. V.; Robotham, S. A.; Bachman, J. L.; Zhong, Y.; Brodbelt, J. S.; Anslyn, E. V., Click and chemically triggered declick reactions through reversible amine and thiol coupling via a conjugate acceptor. *Nat. Chem.* **2016**, *8* (10), 968-973.
22. Johnson, A. M.; Anslyn, E. V., Reversible Macrocyclization of Peptides with a Conjugate Acceptor. *Org. Lett.* **2017**, *19* (7), 1654-1657.
23. Sun, X.; Anslyn, E. V., An Auto-Inductive Cascade for the Optical Sensing of Thiols in Aqueous Media: Application in the Detection of a VX Nerve Agent Mimic. *Angew. Chem. Int. Ed.* **2017**, *129* (32), 9650-9654.
24. Sun, X.; Shabat, D.; Phillips, S. T.; Anslyn, E. V., Self-propagating amplification reactions for molecular detection and signal amplification: Advantages, pitfalls, and challenges. *J. Phys. Org. Chem.* **2018**, DOI: 10.1002/poc.3827.
25. Sun, X.; Boulgakov, A. A.; Smith, L. N.; Metola, P.; Marcotte, E. M.; Anslyn, E. V., Photography Coupled with Self-Propagating Chemical Cascades: Differentiation and Quantitation of G- and V-Nerve Agent Mimics via Chromaticity. *ACS Cent. Sci.* **2018**, *4* (7), 854-861.
26. Ishibashi, J. S. A.; Kalow, J. A., Vitrimeric Silicone Elastomers Enabled by Dynamic Meldrum's Acid-Derived Cross-Links. *ACS Macro Lett.* **2018**, *7* (4), 482-486.
27. Ben Cheikh, A.; Chuche, J.; Manisse, N.; Pommelet, J. C.; Netsch, K. P.; Lorencak, P.; Wentrup, C., Synthesis of alpha-cyano carbonyl compounds by flash vacuum thermolysis of (alkylamino) methylene derivatives of Meldrum's acid. Evidence for facile 1, 3-shifts of alkylamino and alkylthio groups in imidoalkene intermediates. *J. Org. Chem.* **1991**, *56* (3), 970-975.
28. Meadows, M. K.; Sun, X.; Kolesnichenko, I. V.; Hinson, C. M.; Johnson, K. A.; Anslyn, E. V., Mechanistic studies of a "Declick" reaction. *Chem. Sci.* **2019**, *10* (38), 8817-8824.
29. Bräse, S.; Banert, K., *Organic Azides: Syntheses and Applications*; Wiley: Chichester, U.K., 2010.
30. Chawla, K. K.; Meyers, M., *Mechanical behavior of materials*. Prentice Hall: 1999.
31. Zheng, Y.; Li, S.; Weng, Z.; Gao, C., Hyperbranched polymers: advances from synthesis to applications. *Chem. Soc. Rev.* **2015**, *44* (12), 4091-4130.
32. Oliva, N.; Conde, J.; Wang, K.; Artzi, N., Designing Hydrogels for On-Demand Therapy. *Acc. Chem. Res.* **2017**, *50* (4), 669-679.
33. Zhu, Z.; Yang, C. J., Hydrogel Droplet Microfluidics for High-Throughput Single Molecule/Cell Analysis. *Acc. Chem. Res.* **2017**, *50* (1), 22-31.
34. Förster, S.; Antonietti, M., Amphiphilic block copolymers in structure - controlled nanomaterial hybrids. *Adv. Mater.* **1998**, *10* (3), 195-217.
35. Rösler, A.; Vandermeulen, G. W.; Klok, H.-A., Advanced drug delivery devices via self-assembly of amphiphilic block copolymers. *Adv. Drug Deliv. Rev.* **2001**, *53* (1), 95-108.
36. Alexandridis, P.; Lindman, B., *Amphiphilic block copolymers: self-assembly and applications*. Elsevier: 2000.
37. Markoski, L.; Thompson, J.; Moore, J., Indirect Method for Determining Degree of Branching in Hyperbranched Polymers. *Macromolecules* **2002**, *35* (5), 1599-1603.
38. Mohapatra, H.; Phillips, S. T., Using Smell To Triage Samples in Point-of-Care Assays. *Angew. Chem. Int. Ed.* **2012**, *51* (44), 11145-11148.

Insert Table of Contents artwork here

